DOE/MC/29061-96/C0674

CONF-9510109--23

Premixed Burner Experiments: Geometry, Mixing, and Flame Structure Issues

RECEIVED
APR 09 1996
OSTI

Author:

Ashwani K. Gupta
Mark J. Lewis
Maneesh Gupta
Adeboyejo A. Oni
Qua Brown

Contractor:

South Carolina Energy Research and Development Center
Clemson University
Clemson, SC 29634

Contract Number:

DE-FC21-92MC29061
Subcontract No. 94-01-SR028

Conference Title:

Advanced Turbine Systems Annual Program Review

Conference Location:

Morgantown, West Virginia

Conference Dates:

October 17-19, 1995

Conference Sponsor:

U.S. Department of Energy, Office of Power Systems Technology,
Morgantown Energy Technology Center

Contracting Officer Representative (COR):

Norman Holcombe

MT

Disclaimer

P21

Premixed Burner Experiments: Geometry, Mixing, and Flame Structure Issues

Ashwani K. Gupta (akgupta@eng.umd.edu; 301-405-5276)
Mark J. Lewis (lewis@eng.umd.edu; 301-405-1133)
Maneesh Gupta (mgupta1@eng.umd.edu; 301-405-1151)
University of Maryland
Department of Mechanical Engineering
College Park, MD 20742

Adeboyejo A. Oni (oni@bach.eng.morgan.edu; 410-319-3106)
Qua Brown (qbrown@eng.morgan.edu; 410-319-3249)
Morgan State University
School of Engineering
Baltimore, MD 21239

Abstract

This research program is exploring techniques for improved fuel-air mixing, with the aim of achieving combustor operations up to stoichiometric conditions with minimal NO_x and maximum efficiency. The experimental studies involve the use of a double-concentric natural gas burner that is operable in either premixed or non-premixed modes, and the system allows systematic variation of equivalence ratio, swirl strength shear length region and flow momentum in each annulus.

Flame structures formed with various combinations of swirl strengths, flow throughput and equivalence ratios in premixed mode show the significant impact of swirl flow distribution on flame structure emanating from the mixedness. This impact on flame structure is expected to have a pronounced effect on the heat release rate and the emission of NO_x. Thus, swirler design and configuration remains a key factor in the quest for completely optimized combustion.

Parallel numerical studies of the flow and combustion phenomena were carried out, using the RSM and the k-ε turbulence models. These results have not only indicated the strengths and limitations of CFD in performance and pollutants emission predictions, but have provided guidelines on the size and strength of the recirculation produced and the spatio-temporal structure of the combustion flowfield.

The first stage of parametric studies on geometry and operational parameters at Morgan State University have culminated in the completion of a one-dimensional flow code that is integrated with a solid, virtual model of the existing premixed burner. This coupling will provide the unique opportunity to study the impact of geometry on the flowfield and vice-versa, with particular emphasis on concurrent design optimization.

Introduction

Current worldwide emphasis on environmental pollution reduction has resulted in more stringent NO_x emission

Research sponsored by the U.S. Department of Energy's Morgantown Energy Technology Center, under contract 94-01-SR028, with the University of Maryland, College Park, MD, 20742. Fax: 301-314-9477 and Morgan State University, Baltimore, MD 21239. Fax: 410-319-3843.

standards for stationary gas turbine combustion systems in addition to aircraft gas turbines[1]. Lean premixed combustion is receiving wide acceptance since this approach provides the lowest NO_X for combustor operations at any equivalence ratio and power setting. In addition, lean premixed combustion of gaseous fuel provides the most promising technology for CO emission control.

The key in premixed combustion is that the mixture must be adequately mixed at the microscopic level. In addition, constraints that must be met by a realistic mixer include: (1) geometry of the premixer in the fuel preparation tube (i.e., must design for minimum size and pressure drop, in order to avoid back flow during transient operation); (2) efficient method of fuel injection and mixing with the air so that gas residence time exceeds fuel ignition delay time[2] for autoignition; and (3) flame stabilization device (i.e., swirlers) effects on thermal non-uniformity of the flowfield and associated instabilities.

In industrial combustors, the fuel may not burn completely, and may mix and react with the air injected into the primary zone. This situation can lead to the formation of a diffusion flame[3] between the incoming air and the excess fuel or between the excess air in lean zones and excess fuel in rich zones. In this case the temperature of the burned gases is sufficiently high to allow ignition of the mixture. In order to address the above issues, one must examine the isolated effects of each parameter so that the subsequent controlling parameters may be determined for optimal design of combustor operation.

This research program is aimed at developing an understanding of techniques for improved fuel-air mixing, with the aim of achieving combustor operations over a wide range of stoichiometry (up to the limit of stoichiometric conditions) with minimal NO_X and maximum efficiency.

The experimental studies involve the use of a double concentric burner which allows systematic variation of equivalence ratio, swirl strength and flow momentum in each annulus as well as variation of shear between the two annuli. The facility permits combustor operations in both non-premixed and premixed modes. This flexibility allows for the comparison of results obtained in our previous systematic studies on non-premixed flames.

Results have been obtained on the structure of flames formed with various combinations of swirl strengths, flow throughput and equivalence ratios. Specifically, the dynamics of flow field, mean and temporal thermal signature, gas species concentration, mixture fraction distribution and global flame behavior have been examined for the purpose of determining their effects on combustion efficiency and pollutants emission.

The results show that swirl and flow distribution have a significant effect on the size and shape of flames produced, which in turn have a pronounced effect on the heat release rate and the emission of pollutants. The flame structure is controlled, in part, by flow disturbances associated with the swirlers; once these disturbances propagate downstream of the swirler, results show that there is a circumferential non-uniformity of the flame, with attendant consequences on pollutant emissions. Thus, swirler design and configuration remains a key factor in the quest for the fully optimized premixed combustor.

Direct comparisons of the premixed flame data results with the non-premixed flame data showed the compactness of the premixed flames. Furthermore, the flame dimension provided an indication on the quality of mixing. Correlations of flame temperatures indicated a 30% reduction in peak temperatures with premixed flames in comparison to the non -premixed flames. Uniform and lower overall temperatures obtained in premixed flames reveal reduction in the thermal NO_X formation.

The first stage of parametric studies on geometry and operational parameters at Morgan State University have focused on the development and refinement of a one-dimensional flow code that is integrated with a solid, virtual model of the existing premixed burner experimental facility. This one - dimensional flow code development activity has been completed. Driving the geometric design process concurrently with this code will ultimately provide the capability to study the impact of geometry on the flowfield and vice-versa, with particular emphasis on concurrent design optimization whose objective function is tied closely to emissions abatement.

Experimental Studies

Description of the Burner

A schematic diagram of the experimental premixed burner and flow schematic is shown in Figure 1. Methane was used as the fuel. The facility permits various concentrations of fuel and air to be mixed and introduced into the central jet, annulus 1 and annulus 2. The fuel -air mixture ratio in each of these three annuli can thus be varied independently of each other. This provides the required operational flexibility. Before entering the annulus 1 and annulus 2 the incoming fuel-air mixtures are split into four streams. Flame arrestors made of sintered stainless steel (porous plates) are placed inside each jet of the burner. This prevents the pre-mixed flame from propagating upstream of the burner in addition to facilitating the mixing of the reactants. The swirlers create a angular momentum that enhances mixing and creates a stabilizing recirculation zone for the flame. Swirlers are provided for both outer annuli 1 and 2 . The shear layer length between annuli 1 and 2 are changed by using quartz tubes placed at downstream exit of the burner. This also provided optical access to within the flame, inside the burner.

No swirl is used in the central jet. Swirl of any desired strength can be introduced into annulus 1 and 2 by using a pre-fabricated swirler assembly. This allows for investigation with any combination on the radial distribution of swirl in the burner. Eighteen flat vanes made of sheet metal are used for each swirler. This large number of vanes increases the swirler efficiency. The annulus 1 swirler blades are shorter than the annulus 2 due to vane angle manufacturing constraints. Both swirlers are at the same height in the burner.

A traversing mechanism is used to obtain temperature measurements at different spatial locations in the flame. The experimental data presented here is for a premixed case having no swirl in central jet, a swirler vane angle of 30^o in annulus 1, and 55^o in annulus 2, and equivalence ratio of 0.6 in each annulus. Flow rates in annulus 1 and 2 were 11 and 22 scfm, respectively.

Experimental Diagnostics

Information on the global size and shape of the flames obtained with various input and operational parameters were obtained using direct photography. A narrow depth of field and short exposure times were used to obtain tomographic information on the structure of the flame at any desired cross-section of the flow field.

Flow visualization experiments provide information on global instantaneous flame structure. Submicron-sized particles of aluminum oxide were used to enhance the scattered light intensity signal. An averaging technique was used to determine the parameter profiles, which in turn characterizes the mean structure of the flow. Here, information on global turbulence fluctuation of the flow as well as the distribution of the fuel within the flow field was obtained using a laser sheet beam photographic technique.

A CCD camera coupled directly to a PC via an image grabber was used to record the scattered light signal from within the test section. This technique allows for the determination of time mean and standard deviation of fuel fraction distribution within the flow field. The necessary software required for this analysis was developed in our laboratory[4]. This flow visualization experiment provides semi-quantitative information on mixing and concentration of fuel fraction in the flow under both non-burning and burning conditions.

Mean and time-dependent temperature measurements were determined using a 50 µm wire diameter type R thermocouple (Pt-13% Rh). The size of the thermocouple was chosen based on considerations of frequency response, mechanical strength, sensitivity and survivability. This arrangement allows temperature measurement up to the melting point of the thermocouple (1768^{o} C).

Time mean information on temperature was obtained using 300,000 samples over a sampling duration of 30 seconds. This provided a mean data repeatability of better than one percent. However, time-dependent temperature information requires corrections for the thermal inertia associated with the large-size bead thermocouple junction. This in turn requires determination of the time constant of the thermocouple under local prevailing conditions of temperature and flow velocity. This time constant determines the response time to high-frequency changes in the thermal environment. A specially designed electronic circuit was used to determine the time constant of the thermocouple.

In the experiments reported here, temporal and spatial information on the thermal signatures within the premixed flames were obtained to quantify the degree of mixing in flames. Specifically, rms temperature fluctuations, power spectral density, probability density distribution, autocorrelation coefficient, and time scales of microscopic and large-scale turbulence fluctuations were obtained in both premixed and non-premixed flames. The area under the power spectral density - frequency curve is a measure of the variance in the fluctuations of temperature.

The temperature probability density curves are a measure of how closely the temperature data is packed around the mean value. They also give information regarding the nature of the temperature distribution about the mean. The temperature correlation plots give an idea about the microscopic and integral time scales involved in the reaction process. Premixed data show relatively higher values of the microscopic time than the diffusion cases, in certain regions of the flame. This is indicative of large scale eddy mixing of the fuel - air mixtures.

Experimental Results

Global Flame Structure

Results shown in Figure 2(a-c) show significant effects of fuel-air mixture ratio as well as the distribution of reactants within the three annuli on the flame structure. All three flames were obtained with swirl angle in annulus 1 and annulus 2 of 45^{o} and 55^{o}, respectively.

The flame shown in Figure 2(a) was obtained at an equivalence ratio of 0.5 in all three jets. The flame shown in Figure 2(b) was obtained with an equivalence ratio of about 1.0 in all three jets. It is important to note the presence, at this stoichiometry, of large scale structures in the flame that are believed to be caused by the swirlers in the upstream locations of the flame.

Flame photographs shown in Figure 2(c) was obtained with an equivalence ratio of 1.23 in the central jet and 0.52 in annulus 1 and 0.71 in annulus 2. The structure of this flame reveals the presence of a large size central toroidal recirculation zone (in contrast to that obtained for Figures 2(a) and 2(b) despite the identical swirl strength distribution in the combustor. The physical structure of the flame shown in Figure 2(c) appears to be very similar to that obtained from a non-premixed burner in which the fuel is supplied via the central jet.

Temperature Data

Temperature data were obtained with the burner having swirl angle in annulus 1 and annulus 2 of 30^{o} and 55^{o}, respectively. Data were obtained at several spatial locations from within the flame reflecting the central recirculation zone, the shear layer region, outer edge of the flame and the post-flame region, at an equivalence ratio of 0.6, in all three annuli. Sample data are presented in Figure 3, corresponding to spatial locations of r=0; z=1.5, and Figure 4 corresponding to a spatial position of r=1.5; z=1.5.

The results show a gaussian-shaped probability density distribution for temperature measurements in the central region of the flame (see Figure 3). In contrast, a bimodal distribution was obtained for the measurements in the outer shear layer region (see Figure 4). It is important to note that at these two probe volume locations, significant differences have been observed in the integral and microscopic turbulence time scales, and standard deviation of temperature.

The flame behavior in the central core region appears to be dominated by the large scale structures, as evidenced by the large temperature auto-correlation microscopic time scales of about 7.7 ms (Figure 3), as compared to 2.1 ms shown in Figure 4 for the shear layer region.

The integral time scales at these two positions were found to be 130 ms and 2 ms, respectively. The characteristic power spectral density for the shear layer and central core region was found to be several hundred to several kilo- hertz frequency, respectively. This suggests that in the shear layer region, the fuel-air mixture is better-mixed, while in the central core region large scale structures prevail. In an attempt to examine the structure of the flame under non-premixed condition with the same swirl distribution, temperature data were obtained at r=1.5, z=1.5 (see Figure 5).

The non-premixed data, obtained with fuel in the central jet at an overall equivalence ratio of 0.5, shows significant skewness of the temperature probability distribution (see Figure 5). The temperature auto-correlation microscopic time scales as well as the integral time scales were found to be comparable to that of premixed flame (compare auto-correlation coefficients in Figure 4 with those in Figure 5).

Computational Studies

CFD Code and Turbulence Models

The CFD code being used is a general purpose program for modeling fluid flow, heat transfer and chemical reaction. The code can model a wide range of physical phenomena including :

1. 2D/3D geometries in Cartesian, cylindrical or general curvilinear coordinates
2. Turbulent combusting flows
3. Mixing and reaction of chemical species
4. Temperature- and composition - dependent fluid/material properties
5. Incorporation of velocity, heat transfer and non-axisymmetric boundary conditions.

These physical phenomena are modeled by solving the conservation equations for mass, momentum, energy and chemical species using a control volume based, finite difference method. The governing equations are discretized on a curvilinear grid to enable computations in complex, irregular geometries.

A non-staggered system is used for storage of discrete velocities and pressures. Interpolation is accomplished via a first order power law scheme, or optionally, via the higher order QUICK scheme. The equations are solved using the SIMPLEC algorithm with an iterative line-by-line matrix solver and multi-grid acceleration, or with a GMRES full field iterative solver. Numerical solution of turbulent flows without direct simulation requires appropriate modeling procedures to describe the effects of turbulent fluctuations of velocity and scalar quantities in the basic conservation equations. The code used here makes use of either the k-ε or the Reynolds Stress turbulence models.

The major limitations of the k-ε model is that υ_t is assumed to be isotropic. This implies that the velocity and length scales are the same in all the directions. In complex swirling flows velocity and length scales can vary significantly with direction. For such flows, the k-ε model is inadequate and can produce physically incorrect results.

The RSM model computes the individual Reynolds stresses by solving the transport equations for the individual stresses. These transport equations can be derived from the momentum equations and contain triple order velocity correlations and pressure velocity correlations that must be modeled to obtain closure. This involves the modeling of the stress production rate, pressure-strain correlation, and viscous dissipation amongst other parameters.

Performance Prediction

To compare the experimental and computational results, a base line non-premixed case was considered which allowed direct comparison of the experimental and computational profiles. The flames considered are given in Table 1. Case 1 was chosen due to the availability of comprehensive experimental data from our own laboratory.

As seen from the experimental temperature profiles in Figure 6 and the computational temperature profiles in Figure 7, qualitative agreement is obtained. The computational software overpredicts the temperatures throughout the domain by about 100 deg. A two-step reaction scheme and activation of the radiation model may further improve the computational results.

Case 2 is similar to case 1 except that case 2 is a premixed flame. Some of the observations that could be made from the results from case 1 and 2 are as follows:

1. Non-premixed flames (Fig. 8) provide stronger recirculation and lower maximum positive axial velocities near to the burner exit than the premixed flame (see Figures 8 and 9).
2. Azimuthal velocities were almost identical for the two cases
3. On an average, a temperature reduction of 30% is obtained over the entire flow field for the premixed case. The temperature profile for the premixed are more non-uniform at the burner exit
4. Temperature profiles exhibit a different behavior in the expansion zone of the burner for the premixed and non-premixed cases. The temperature profile for the premixed case shows bimodal distribution having distinct peaks away from the burner centerline and a trough at the centerline (see Fig. 10). The profiles develop into a monomod form at an axial station located approximately at $z/D=0.27$, where z is the axial distance measured from the control inlet jet.

The results obtained for the non -premixed case, case 1, have a monomodal appearance throughout the entire combustor length. The bimodal peaks are probably due to the premixed nature of the fuel introduction in the outer two annuli and this effect is observed downstream until the fuel-air mixture attains a more homogenous composition.

The flame in case 3 is a premixed flame having conditions similar to that given for Figure 9 except that an equivalence ratio of 1.0 was used. A comparison between cases 1 and 3 data revealed the following:

1. The recirculation zone is almost non-existent for the premixed case 3 as shown in Figure 11. The maximum positive axial velocities are considerably higher than the non - premixed and the lean premixed cases 1 and 2. The velocity decay is higher for the stoichiometric premixed case 3 as compared to the other non-premixed and premixed cases. The higher axial velocity for case 3 inhibits the growth of a recirculation zone.
2. Maximum temperatures at higher equivalence ratio for the premixed case 3 are comparable to those obtained at lower equivalence ratio for the non-premixed case 1 (compare Figure 12 with Figure 7). Temperatures with the stoichiometric premixed case 3 are about 30% higher than lean premixed case 2 (compare Figure 12 with Figure 10).
3. The bimodal nature of the temperature profiles for the stoichiometric premixed case 3 diminish as compared to the lean premixed case 2 (compare temperature profiles near burner exit in Figures 10 and 12.
4. Significantly higher turbulent transport values are obtained for the stoichiometric

premixed case 3. The exact location and amplitude of these turbulent transport are responsible for improved mixing of the fuel - air mixture.

Analysis of Test Results

Comparison of the computational results for the premixed flames obtained with a systematic variation in the swirl, angular momentum ratio and equivalence ratio is now discussed. The following test matrix was considered:

- Flame Type: Premixed flame
- Total equivalence ratio : 0.5 and 1.0
- $[Q_{ann1}/Q_{ann2}]$: 0.5 , 1.0
- Swirl vane angle in annulus 1/annulus 2: 00/55, 45/55, 60/00, 60/35 degrees.

Impact of Swirl Flow Distribution

1. For all premixed cases the swirl vane angle in annulus 1 and annulus 2 had only a small effect on the size and strength of the recirculation zone.
2. The bimodal nature of the temperature profiles is most pronounced for the case with no swirl in annulus 1. With an increase in the swirl angle in annulus 1, this effect subsides. The temperature field was, in general, insensitive to the strength and distribution of swirl. This information requires verification
3. Turbulent kinetic energy levels increase with an increase in swirl vane angles in annulus 1 (compare Figure 13 with Figure 14 corresponding to cases 4 and 5, respectively).

Impact of Angular Momentum Ratio

The following observations were made when the flow ratios in the two annuli, $[Q_{ann1}/Q_{ann2}]$, were varied from 0.5 to 1:

1. A small increase in strength of the recirculation zone for equal flow in the two annuli as compared to the condition with higher flow in annulus 2.
2. Temperature field is insensitive to the variations in flow rates in the two annuli.
3. Figures 14 and 15 show that the turbulence kinetic energy increases by almost 100 % as the flow ratio is varied from 0.5 to 1. This finding may serve as a valuable aid to develop new mixing strategies.

Implications of Equivalence Ratio Variations

The following observations can be made from the studies carried out by varying the equivalence ratio from 0.5 to 1 :

1. Decreased size of the recirculation zone at higher equivalence ratios
2. Figures 16 and 17 show that higher values of azimuthal velocities are obtained at the higher equivalence ratios. Theoretically, this should lead to a well defined recirculation zone. The k-ε model is well known for underpredicting the strength of the recirculation zone. The RSM model may assist to capture this effect.
3. Mean temperatures decrease by almost 30% when the equivalence ratio is decreased from 1 to 0.5. Also the temperature profiles no longer have a monomodal appearance for the case of an equivalence ratio equal to 0.5.

Summary

The results presented here have shown a significant effect of the radial distribution of swirl on the degree of mixing and structure of premixed flames. Experimental data reveals that premixed flames can have large time integral scales in certain regions of the flame. The degree of mixing and flame structure are significantly affected by the presence of swirlers in the flow. The nonuniformity of thermal field is different in different regions of the flow field. Premixed flames at higher equivalence ratios yielded decreased size and strength of the central toroidal recirculation zone. Premixed flames yielded uniform and lower overall flame temperatures so that carefully mixed (premixed) flames have the most potential for reduced pollutants emission from flames. These results are of direct benefit in the design and development of gas turbine combustors, particularly for achieving higher efficiencies and low pollution.

Future Activities

Our future activities will focus on a closer examination of the regions that contribute to NO_X by examining in detail, the structure of the flames, non-intrusively, complimented with numerical calculations. Our immediate goal will be to provide a comprehensive mapping of these specific flames, with a view to correlating time scales with the propensity for NO_X generation.

Acknowledgments

The research support provided here is gratefully acknowledged. Technical support, assistance and collaboration provided by Pratt & Whitney, East Hartford, CT is deeply appreciated. We also acknowledge the assistance of DOE Project Managers Dr. Paul Micheli and Dr. Norm Holcombe, and also the ATS Research Manager, Dr. Daniel Fant. Technical assistance on this project was provided by Messrs Andre' Marshall, Song Qi, Robert Aftel and Harald Kafitz.

References

1. Gupta, A.K. and D.G. Lilley: Combustion and Environmental Challenges for Gas Turbines in the 1990s. AIAA Paper 91-1964.
2. Spadaccini, L.J. and J.A TeVelde: Autoignition Characteristics of Aircraft-Type Fuels, Combustion and Flame, Vol. 46, 1982, pp 283-300.
3. Libby, P.A. and F.A. Williams: *Turbulent Reaction Flows*, Academic Press, 1994.
4. Marshall, A : Ph.D Thesis (in progress), Department of Mechanical Engineering, University of Maryland, 1996.

Table 1. Test Matrix for the Presented Data

Case No	Flame Type	Swirl Vane Angle (deg.) Annulus 1	Annulus 2	Flow Rates (SCFM) Annulus 1	Annulus 2	Equivalence Ratio
1	Non-premixed	45	55	11	22	0.5
2	Premixed	45	55	11	22	0.5
3	Premixed	45	55	11	22	1.0
4	Premixed	45	55	16.5	16.5	1.0
5	Premixed	60	35	16.5	16.5	1.0
6	Premixed	60	35	11	22	1.0
7	Premixed	60	35	11	22	0.5

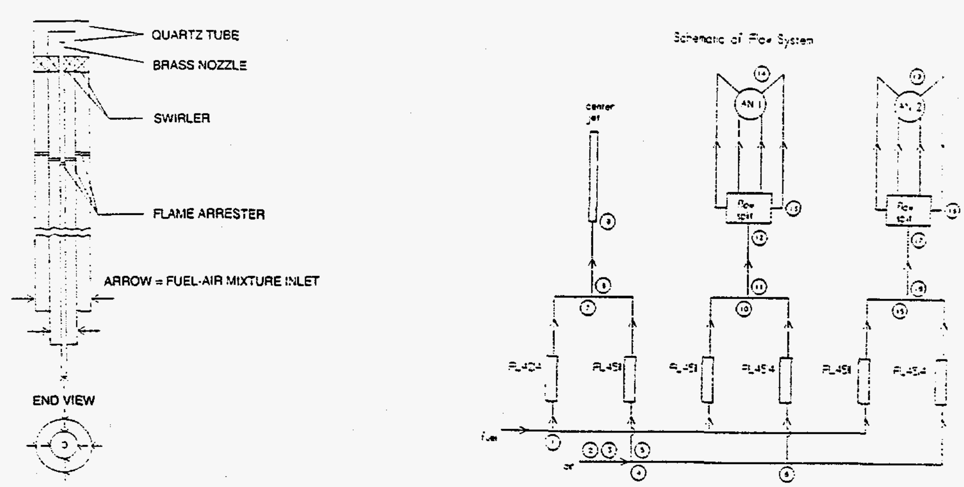

Fig. 1 Diagram of burner and flow delivery system.

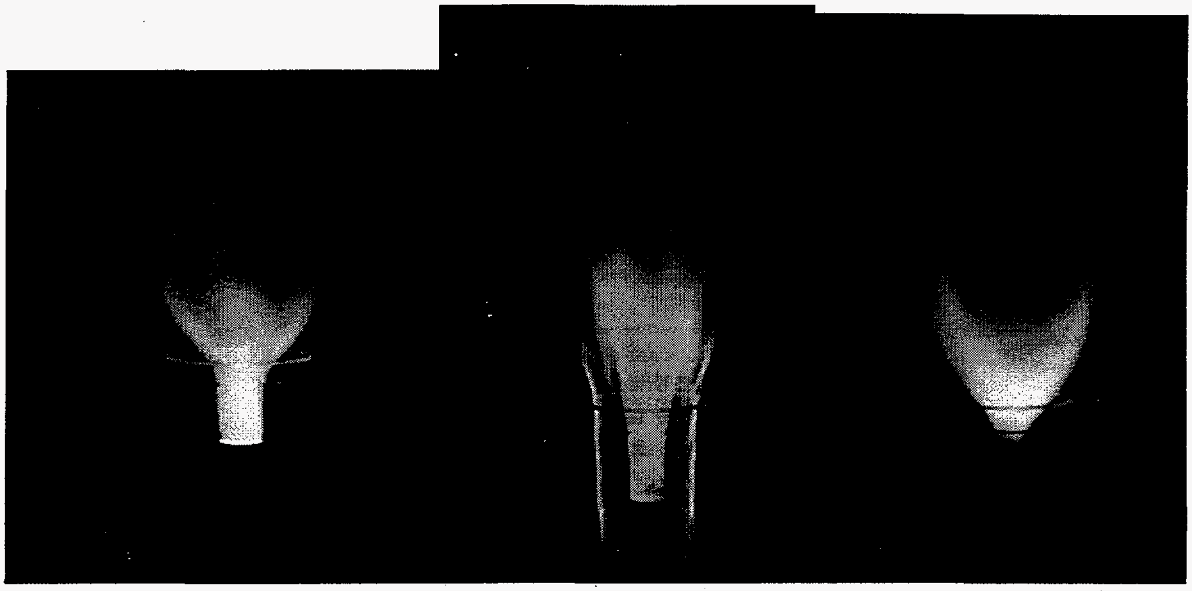

a b c

Fig. 2 (a) Flame photograph with ø = 0.5 in all three jets; (b) Flame photograph with ø = 0.98, 0.94 and 1.06 in central jet, annulus 1 and annulus 2, respectively (overall ø = 1.0); (c) Flame photograph with ø = 1.23, 0.52 and 0.71 in central jet, annulus 1 and annulus 2, respectively (overall ø = 0.65).

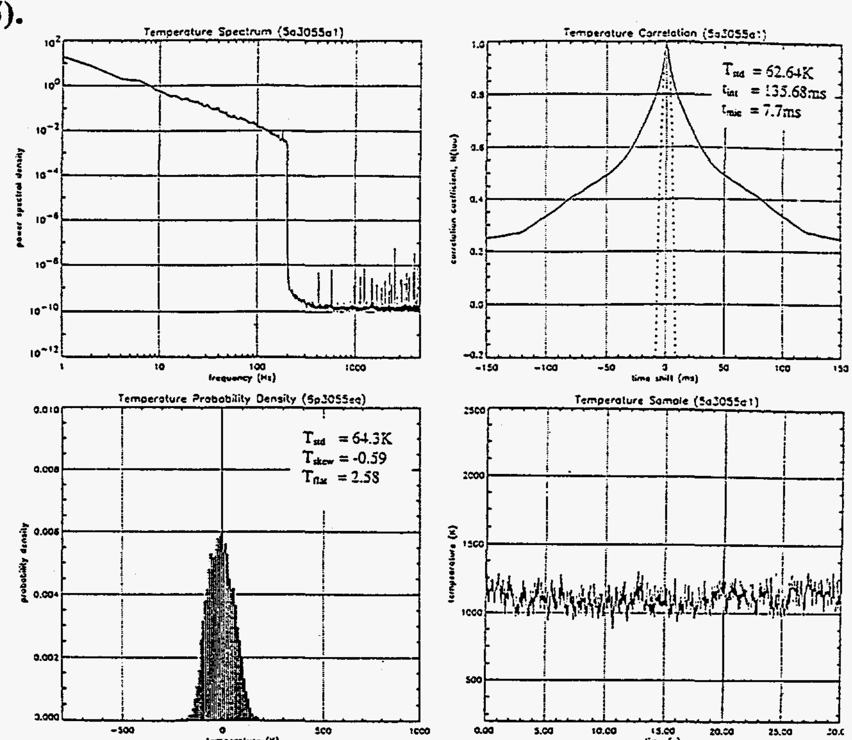

Fig. 3 Power spectral density, autocorrelation coefficient, probability density and temporal variation of temperature in premixed flame at r = 0 and z = 1.5 inches with S1 = 30° in annulus 1 and S2 = 55° in annulus 2. Flow in annulus 2 was twice that in annulus 1.

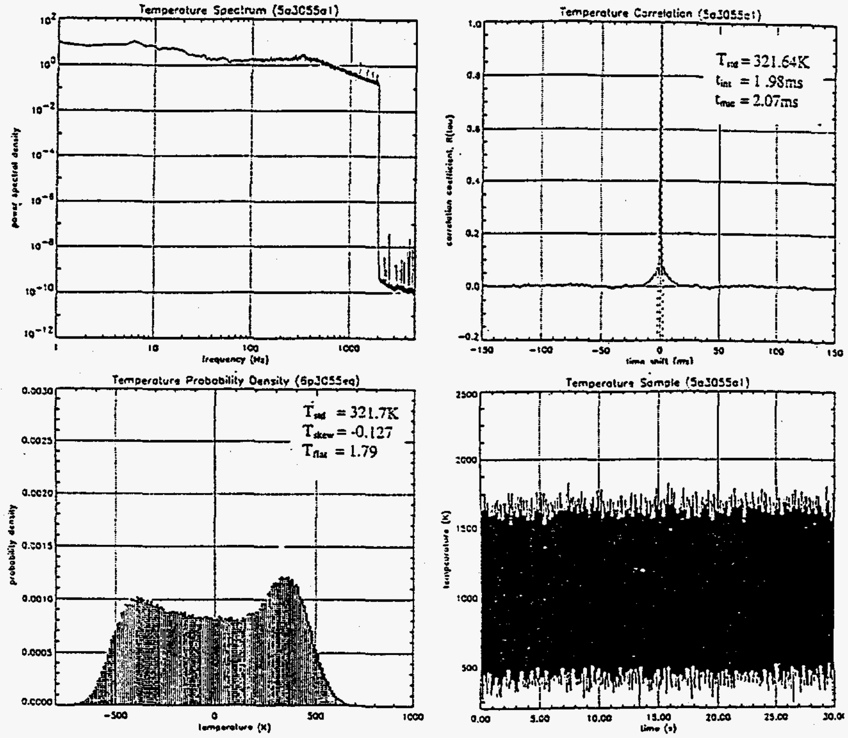

Fig. 4 Power spectral density, autocorrelation coefficient, probability density and temporal variation of temperature in premixed flame at r = 1.5 and z = 1.5 inches. Other conditions are the same as those given for Fig. 3.

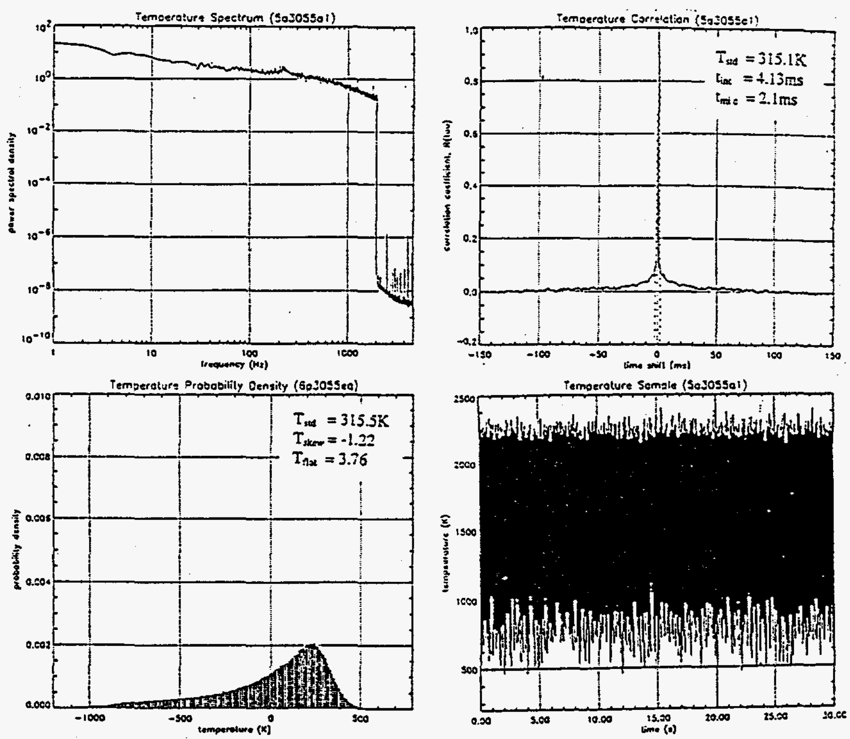

Fig. 5 Power spectral density, autocorrelation coefficient, probability density and temporal variation of temperature in non-premixed flame at r = 1.5 and z = 1.5 inches with S1 = 30°, S2 = 55°. Flow in annulus 1 was the same as that in annulus 2.

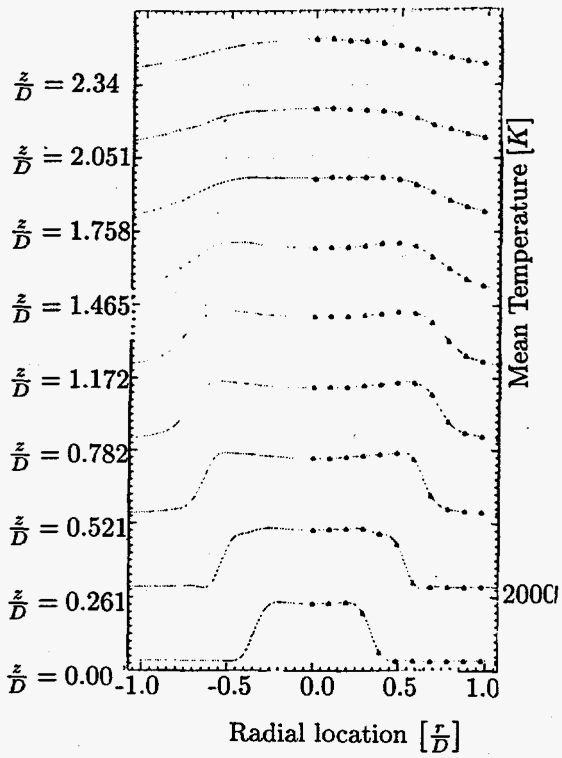

Fig.6. Experimental temperature profiles in non - premixed flame.

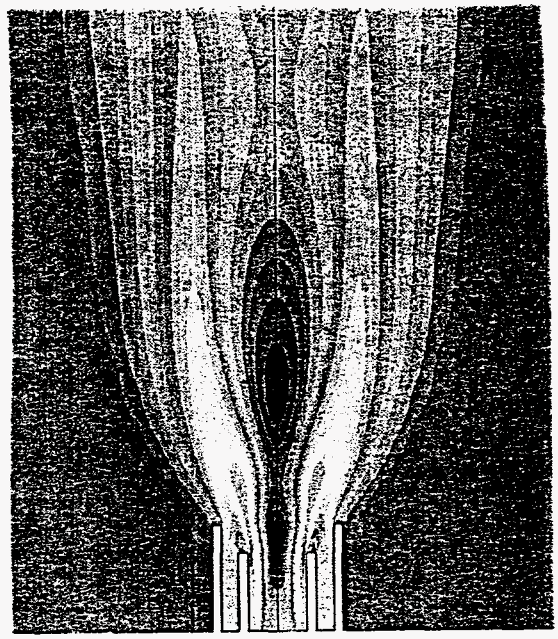

Fig.8. Computational U-velocity profiles for case 1 flame. Scale is 1 unit=3.63 m/sec.

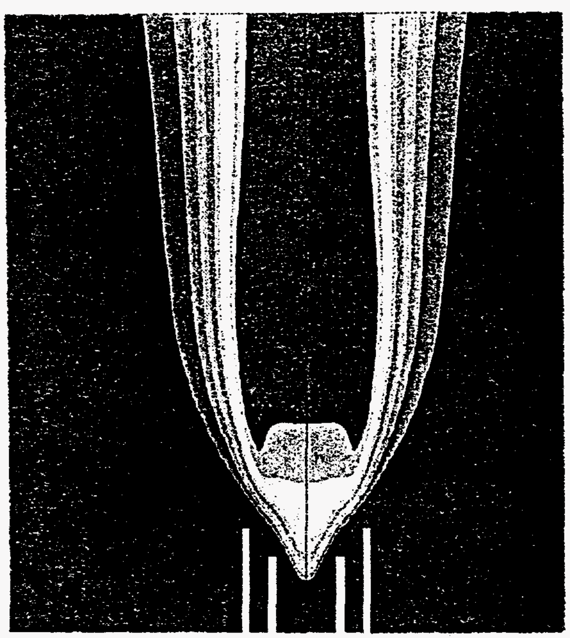

Fig.7. Computational temperature profiles for case 1 flame. Scale is 1 unit=400 K

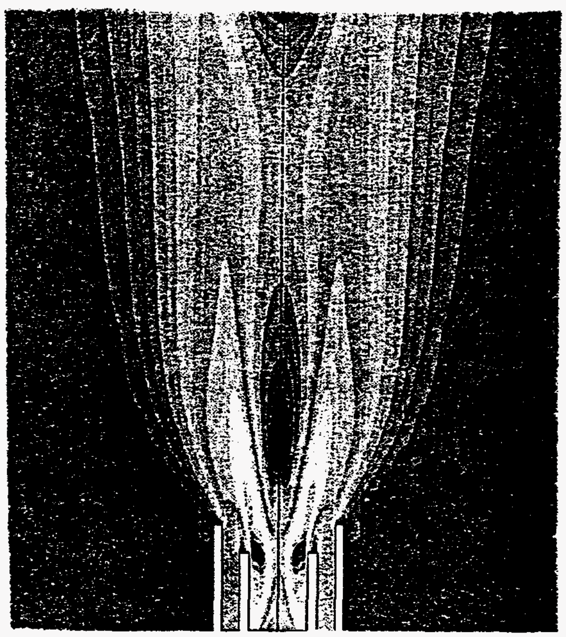

Fig.9. Computational U-velocity profiles for case 2 flame. Scale is 1 unit=3.725 m/sec

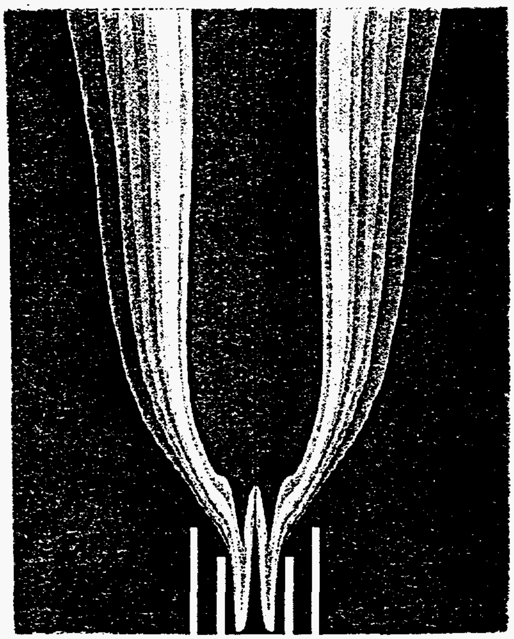

Fig.10. Computational temperature profiles for case 2 flame. Scale is 1 unit= 254 K.

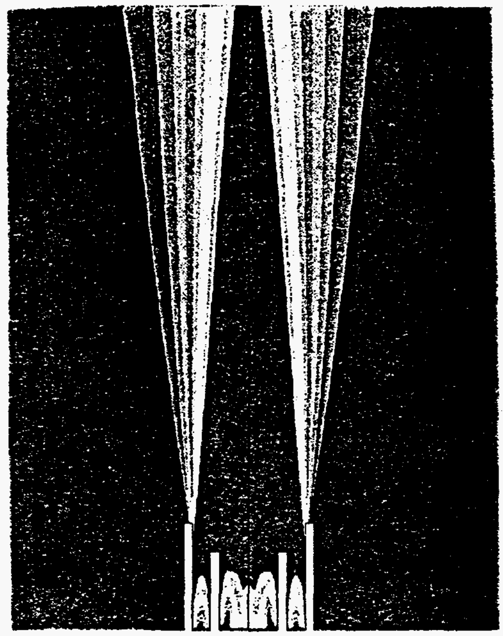

Fig.12. Computational temperature profiles for case 3 flame. Scale is 1 unit = 402 K.

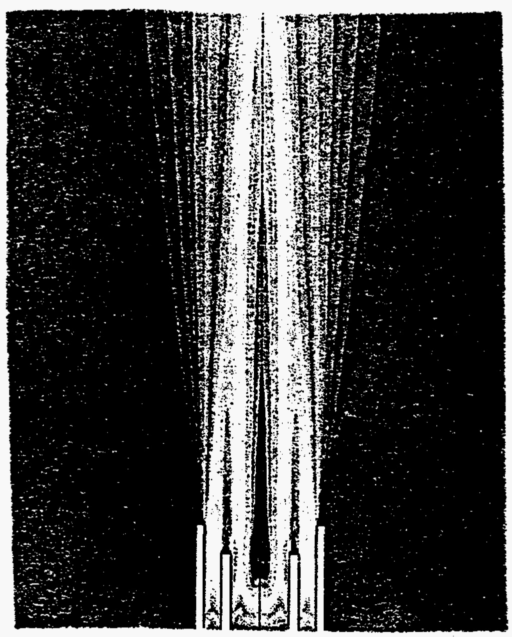

Fig.11. Computational U-velocity profiles for case 3 flame. Scale is 1 unit= 13.9 m/s

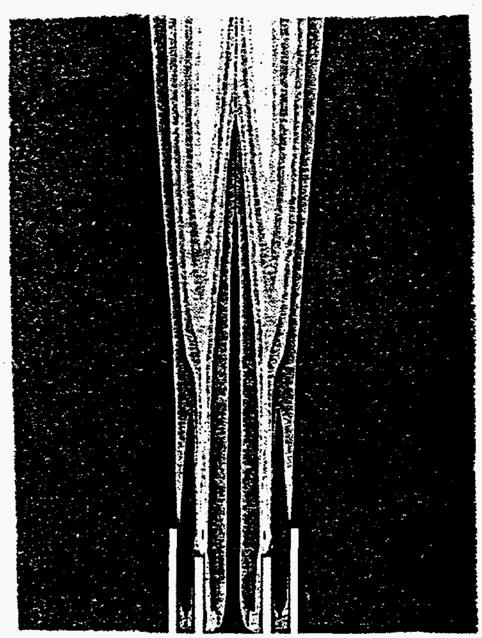

Fig.13. Computational turbulent kinetic energy profiles for case 4 flame. Scale is 1 unit = 67.5 m/s.

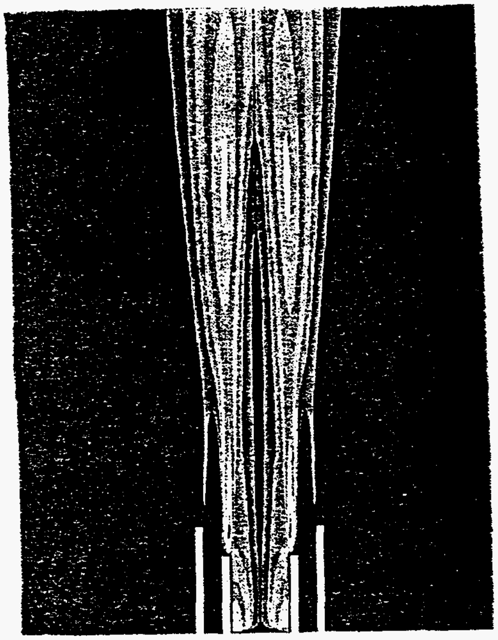

Fig.14. Computational turbulent kinetic energy profiles for case 5 flame. Scale is 1 unit = 89.5 m/s

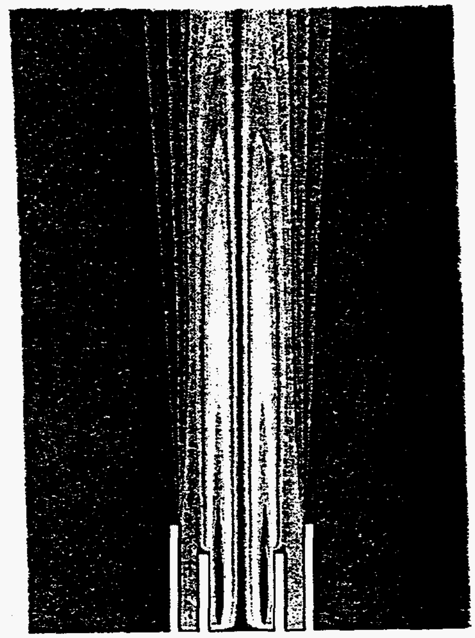

Fig.16. Computational azimuthal velocity plots for case 6 flame. Scale is 1 unit = 4.4 m/s

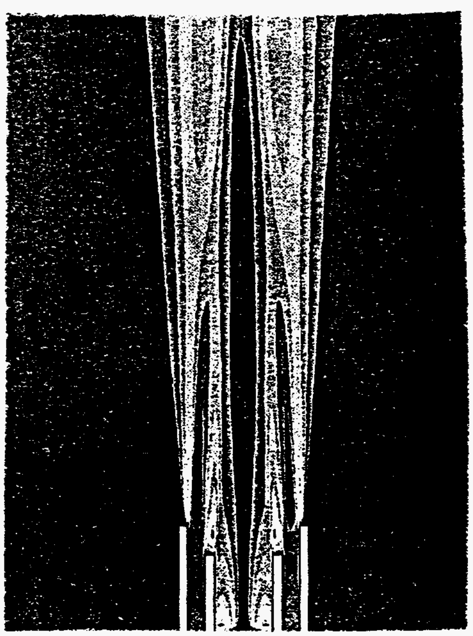

Fig.15. Computational turbulent kinetic energy profiles for case 6 flame. Scale is 1 unit = 42.75 m/s

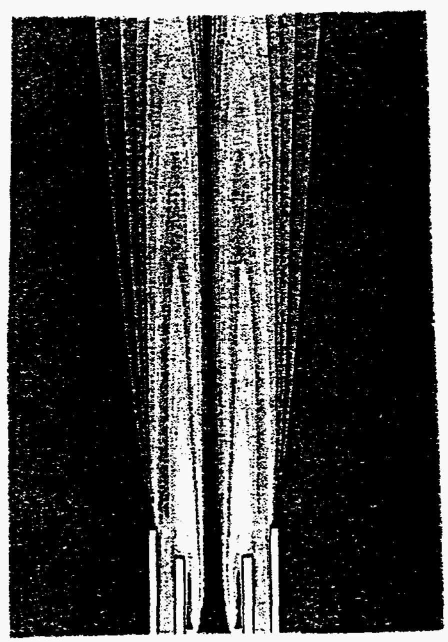

Fig.17. Computational azimuthal velocity plots for case 7 flame. Scale is 1 unit = 4.45 m/s